Block commutation vs. FOC in power tool motor control

About this document

Scope and purpose

This application note provides a side-by-side comparison of block commutation control and Field-Oriented Control (FOC) for three-phase Brushless Direct Current (BLDC) motors in power tool applications, and it should provide information to the reader about the benefits of each method, supporting a possible decision between them on a real motor drive application. The document first gives an overview of block commutation control and sensorless FOC, then compares the hardware and software requirements. Finally it shows real test results of both methods.

Intended audience

Sales and Field Application Engineers (FAEs), motor control engineers, power electronics engineers, power tool designers and manufacturers.

Table of contents

About this document **1**
Table of contents **2**
1 Introduction **3**
2 Hardware comparison **4**
2.1 Hardware for block commutation with Hall sensors 4
2.2 Hardware for sensorless FOC 5
2.3 Hardware comparison 6
3 Software comparison **8**
3.1 Block commutation algorithm with Hall sensors 8
3.2 Sensorless FOC algorithm 8
3.3 Software comparison 8
4 Test results comparison **11**
4.1 Test set-up 11
4.2 Motor phase current comparison 12
4.3 Power comparison 13
4.3.1 MOSFET power loss comparison 14
4.4 Thermal comparison 15
4.5 Motor start-up comparison 16
5 Summary **17**
6 References **18**
Revision history **19**

1 Introduction

Three-phase BLDC motors have become more and more popular in power tools such as drills, drivers, sanders, grinders and saws. Until now block commutation with Hall sensors has been the dominant control method for three-phase BLDC motors in power tool applications. Block commutation of three-phase BLDC motors is an electronic commutation scheme also known as trapezoidal commutation, six-step commutation or 120-degree commutation. In this control method, each phase conducts for 120 degrees (electrical degrees, see below) during the positive and negative half of a Back-EMF (BEMF) cycle, and is off or un-energized for the remainder of the cycle. This algorithm requires rotor position information for every 60 degrees, and normally three Hall sensors are used to provide the rotor position feedback.

FOC, also known as vector control, is an advanced motor control method to generate three-phase sinusoidal signals that can be controlled in frequency and amplitude in order to minimize the current, which means maximizing the power efficiency. The basic idea is to transform three-phase signals into two rotor-fixed signals, execute control algorithms and transform back to a three-phase system. Feedback on rotor position is also needed by a FOC motor control.

With increased CPU performance, sensorless FOC has been made possible for three-phase motor control in power tool applications. Sensorless FOC doesn’t require any rotor position or speed sensors (e.g. Hall sensors, encoders or resolvers); instead, a software sensorless estimator is used to calculate the rotor position and rotor speed.

This document focuses on the comparison of block commutation with Hall sensors versus sensorless FOC in a specific application of three-phase BLDC motor control for power tools, mainly to help the reader decide which method is best suited to their application. Detailed descriptions of block commutation with Hall sensors, sensorless FOC and three-phase BLDC motors are beyond the scope of this application note. Please refer to the documents in the reference section for more details.

2 Hardware comparison

2.1 Hardware for block commutation with Hall sensors

The block diagram of the hardware design for block commutation with Hall sensors is shown in Figure 1.

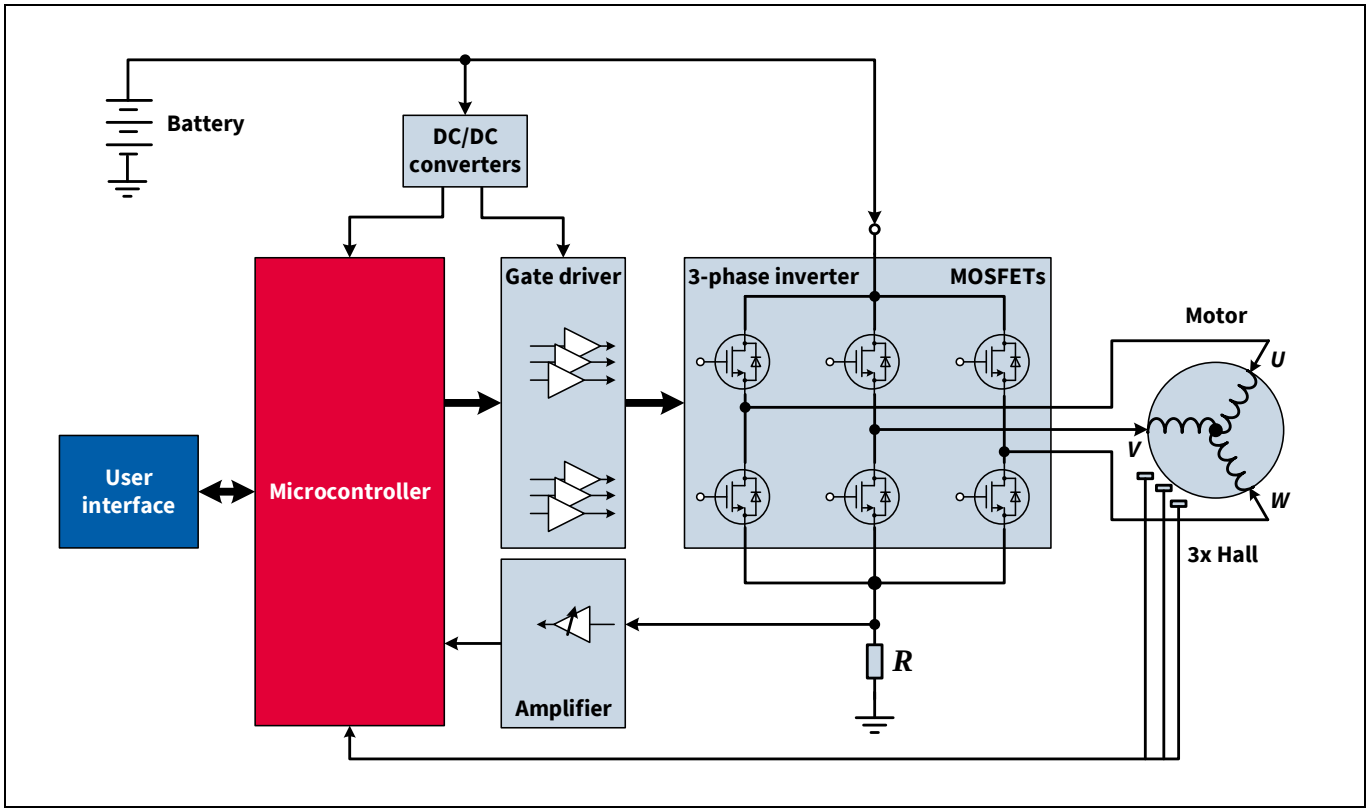

Figure 1 Block diagram of block commutation hardware

2.2 Hardware for sensorless FOC

The block diagram of hardware design for sensorless FOC is shown in Figure 2.

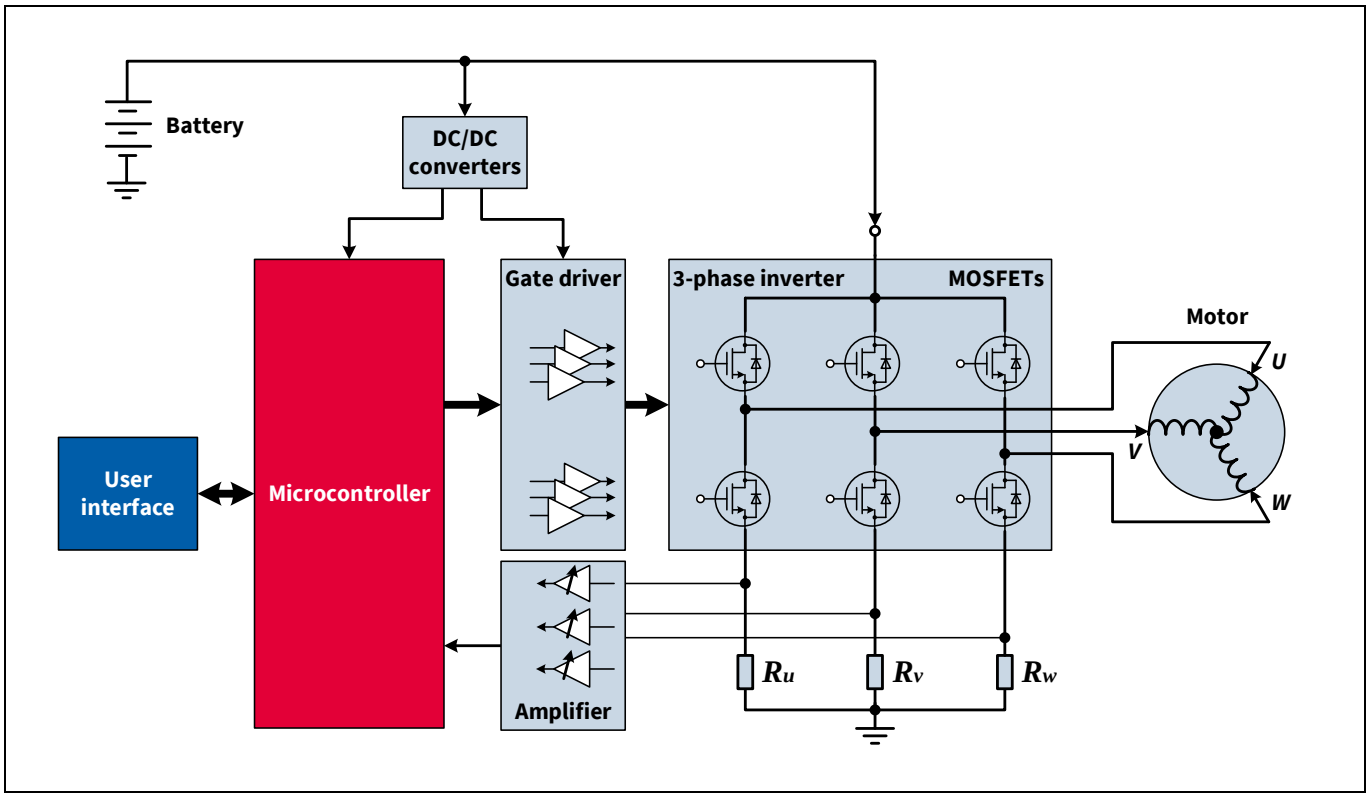

Figure 2 Block diagram of sensorless FOC hardware

2.3 Hardware comparison

Table 1 is a comparison of typical hardware design of BLDC block commutation with Hall sensors and sensorless FOC.

Table 1 Comparison of typical hardware of block commutation with Hall and sensorless FOC

Item	Block commutation	Sensorless FOC	Comments
Three-phase inverter	Six MOSFETs	Six MOSFETs	Normally all N-channel power MOSFETs, e.g. IRF7480MTRPbF, IRL40T209, BSC010N04LSI, etc.
Gate driver	Three half-bridge gate drivers	Three half-bridge gate drivers	
MCU	Low calculation power needed	More calculation power needed	Low power consumption becomes essential
Typical power supply for gate driver	+12 V	+12 V	Other possible voltages: +7 V, +9 V, +15 V, etc.
Typical power supply for microcontroller	+5 V, from buck converter or LDO 3.3 V possible	+5 V, from LDO is highly preferred	Accuracy requirement in FOC is higher due to precision needed for current sensing. Other possible voltage: +3.3 V. However, 5 V provides more resolution per ADC Least Significant Bit (LSB). Therefore 5 V is preferred in FOC.
Current sensing	One leg shunt	Three leg shunts High accuracy	
Current sensing amplifiers	One amplifier	Three amplifiers High-performing: slew rate, bandwidth, offset error	
Rotor sensor	Three Hall sensors	None	In FOC Hall sensors are eliminated by using a software estimator instead.

There are common hardware elements for block commutation with Hall sensors and sensorless FOC. These are the three-phase inverter, gate drivers, MCU and power supplies for the ICs.

The three-phase inverter's switching devices are normally N-channel power MOSFETs for battery-powered power tool applications. During the switching, dead-time is inserted into the Pulse Width Modulation (PWM) signals to prevent the high-side and low-side MOSFETs of each inverter leg being on at the same time (i.e. shoot-through). The body diode of each MOSFET helps conduct current whenever necessary when the MOSFET is off. Two or more MOSFETs in parallel for each of the MOSFETs are commonly used to achieve higher output power. Heatsinks may be needed to extract heat efficiently from the power MOSFETs depending on the power tool's power rating, electronic board design, mechanical design or thermal design.

Hardware comparison

Gate drivers serve as the interface between control signals of the MCU and MOSFETs. Gate drivers output the right voltage and current level to drive the gates of the MOSFETs effectively and efficiently in this PWM switching application. The input signals of gate drivers are from the PWM unit of the MCU. The MCU also executes the algorithms of block commutation with Hall sensors or sensorless FOC to control the three-phase BLDC motor.

For battery-powered power tool applications, the power supplies are from the battery. Switching regulators, Low-Dropout Regulators (LDOs) or charge pumps are used to generate stable DC voltages for the ICs, e.g. +5 V for MCU, +12 V for gate driver ICs. To save battery power, it is desirable to choose semiconductor components with low power consumption.

Typically block commutation with Hall sensors uses one shunt to sense the current of the DC link. For rotor speed and position estimation, it needs three Hall sensors and corresponding cables, connectors and PCB for the Hall sensors.

Sensorless FOC doesn’t require Hall sensors and normally uses three shunts to sense the motor phase current. For rotor speed and position estimation, it uses a sensorless estimator. Accurate motor phase current sensing is very important to achieve precise rotor speed and position estimation. One-shunt or two-shunt current sensing in sensorless FOC works for some of the power tool motor control applications (e.g. leaf blower) but they don’t have the same current sensing capability and accuracy as with three-shunt current sensing. One-shunt and two-shunt current sensing for sensorless FOC is not considered in this application note.

3 Software comparison

3.1 Block commutation algorithm with Hall sensors

The block diagram of a typical BLDC block commutation with Hall sensors is shown in Figure 3. More details of BLDC block commutation can be found in [1].

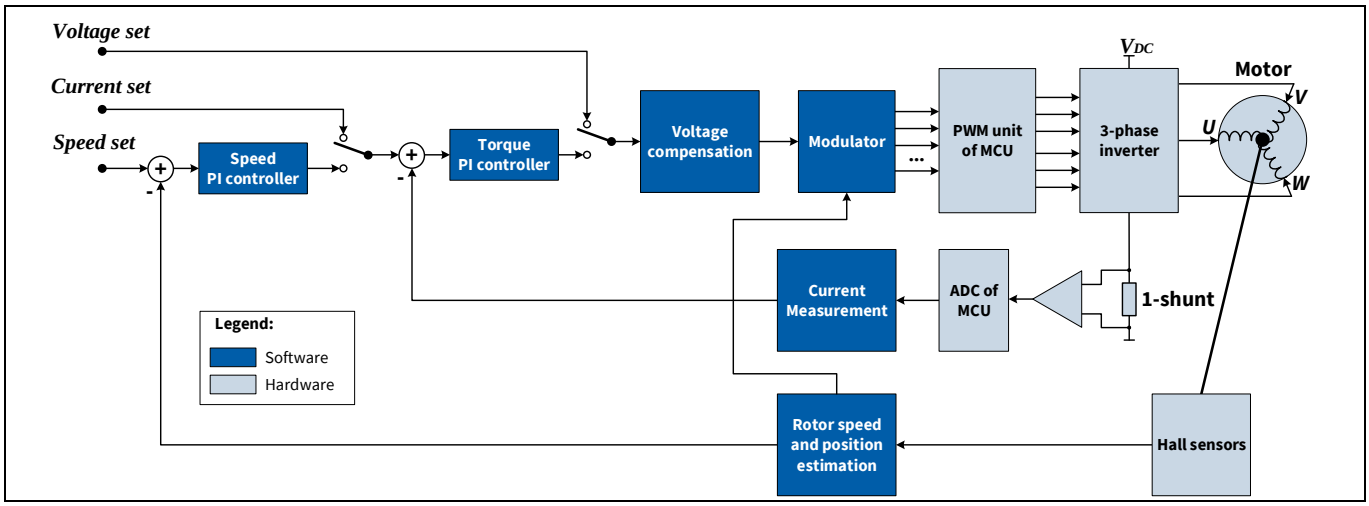

Figure 3 Block diagram of block commutation algorithm

3.2 Sensorless FOC algorithm

The block diagram of a typical sensorless FOC is shown in Figure 4. More details of sensorless FOC can be found in [2].

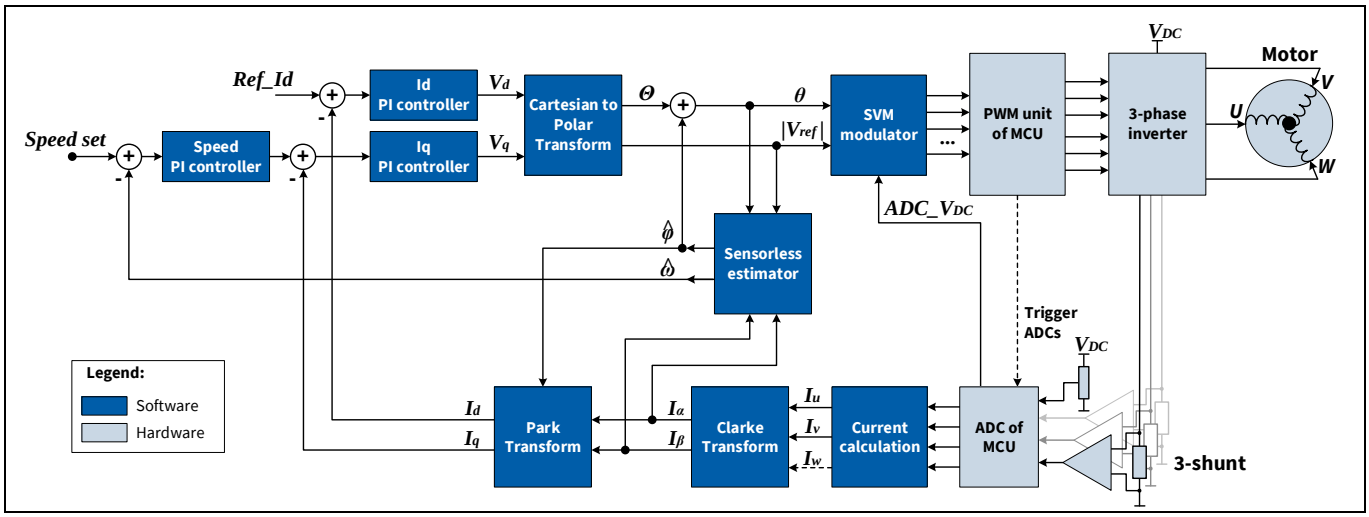

Figure 4 Block diagram of sensorless FOC algorithm

3.3 Software comparison

Table 2 is a comparison of the control software algorithms of BLDC block commutation with Hall sensors and sensorless FOC.

Software comparison

Table 2 Comparison of control algorithms of block commutation with Hall and sensorless FOC

Item	Block commutation	Sensorless FOC	Comments
Number of energized phases during motor operation	Two phases	Three phases	
Positions of stator magnetic flux vectors	Six fixed positions	Infinite – continuous movement of vector	
Angle between rotor and stator fluxes	Continuously varying between 60 degrees and 120 degrees when the rotor advances	Maintain 90 degrees (or close to 90 degrees) all the time	
Preferred motor BEMF	Trapezoidal	Sinusoidal (or close to sinusoidal)	
Current sensing	Average current of DC link of inverter, unidirectional	Instantaneous current of three phases of motor, bidirectional	Sensing from one shunt for block commutation, and three shunts for sensorless FOC
Current sense accuracy	Low	High, requires sampling in short noisy periods for high-speed operation	
Rotor position sensing	Hall signal processing (rotor speed and position estimation)	Software sensorless estimator	Normally three Hall signal processing is used for block commutation
Start-up method	Hall sensor closed-loop start-up	Direct sensorless FOC closed-loop start-up	
Coordinate transformation	–	Clarke transform, park transform, Cartesian-to-polar transform (or inverse park transform)	
PI controllers	Speed, torque (current)	Speed, I_d (flux), I_q (torque) and more	
PWM generation	Requires a good Hall modulator state machine capability in timers like POSIF in XMC™	Benefits from high-resolution PWM	
Algorithm complexity	Low	High, benefits from high-performance MCU or Math coprocessor like MATH in XMC1000	
Execution time of control loop	Shorter execution time (e.g. 10 µs)	Longer execution time (e.g. 21 µs)	
Typical code size	Smaller (e.g. 16 kB)	Larger (e.g. 18 kB)	

Software comparison

Main limitation	Lower power efficiency, higher torque ripple	Difficult to provide high torque at start-up and low speed	

During the motor drive of block commutation, only two motor phases (UV, VW and UW, or VU, WV and WU when the phase current reverses) are energized and the third phase is floating, creating only six possible directions of stator flux vectors. The sensed DC link current is the same current as the two energized phases, and the phase current can be bidirectional but the DC link current is always unidirectional. Meanwhile, for sensorless FOC all the three motor phases are energized and the three-phase current was controlled to be sinusoidal, which can ideally generate infinite directions of stator flux vectors. Also, the instantaneous currents of three motor phases are sensed and they are bidirectional.

The electrodynamic torque can be calculated with the vector cross-product of both the rotor flux and stator current space vector [4]:

$$\overrightarrow{T_e} = \overrightarrow{\Psi_m} \times \vec{\imath} = |\Psi_m||i|\sin(\theta)\vec{n}$$

Where:

- $\overrightarrow{T_e}$ is the electrodynamic torque of the motor, with direction of unit vector $\vec{n}$;
- $\overrightarrow{\Psi_m}$ is the rotor flux of the permanent magnet, with a magnitude of $|\Psi_m|$;
- $\vec{\imath}$ is the stator current space vector, with a magnitude of $|i|$. It represents the stator flux;
- θ is the angle between rotor and stator fluxes.

To obtain maximum torque and efficiency from the BLDC motor, the angle θ between the rotor and stator fluxes is controlled to be 90 degrees (or close to 90 degrees) all the time for sensorless FOC, as it controls stator flux direction (and magnitude) continuously based on rotor flux position. Conversely, for BLDC block commutation with Hall sensors the stator flux rotates in only six possible directions with 60-degree intervals (i.e. six steps per revolution), while the rotor flux rotates continuously. So it is impossible to always keep the angle θ at 90 degrees. θ actually varies between 60 degrees and 120 degrees typically, repeating every 60 degrees as the rotor revolves. Subsequently, its power efficiency is not always maximized.

The above key differences help to explain why the sensorless FOC's torque ripple is lower and power efficiency is higher than BLDC block commutation with Hall sensors. Due to these differences, the requirements of the motor design are different, too. For block commutation with Hall sensors, the motor works well if the BEMF shape is trapezoidal. On the other hand, the motor BEMF is preferred to be sinusoidal (or close to sinusoidal) if sensorless FOC is used.

The BLDC block commutation is relatively simpler and the execution time of the control loop is shorter than sensorless FOC for the same MCU. Sensorless FOC is much more complex and mathematically intensive, and it has time-consuming calculation blocks such as park transform, Cartesian-to-polar transform, sensorless estimator and Space Vector Modulation (SVM), and thus its execution time is normally longer than block commutation for the same MCU.

For block commutation with both Hall sensors and sensorless FOC, the number of Proportional Integral (PI) controllers to be used depends on the application, e.g. for power drills and drivers with high dynamic torque requirements, torque PI controller may be used without speed PI controller; for grinders and leaf blowers all PI controllers (speed, torque, etc.) may be used to control the motor to a relatively constant speed no matter what the load torque is.

4 Test results comparison

4.1 Test set-up

The key parts of a test set-up to compare block commutation with Hall sensors and sensorless FOC are shown in Figure 5.

A power board shown on the left in Figure 6 with a three-phase inverter is to test the two algorithms with the same three-phase BLDC motor with trapezoidal BEMF of the power tool. The heatsink is removed and the power MOSFETs are IRF7480MTRPbF [7]. The detached microcontroller board is shown on the right of Figure 6.

The motor parameters are listed in Table 3. A dynamometer (magnetic brake system) is coupled to the motor shaft to load the motor, and measure the torque, shaft speed and mechanical output power of the motor. A power analyzer can measure the input and output power of the power board. At the same time, a thermal camera is used to monitor the temperature of the board, especially the MOSFETs of the three-phase inverter.

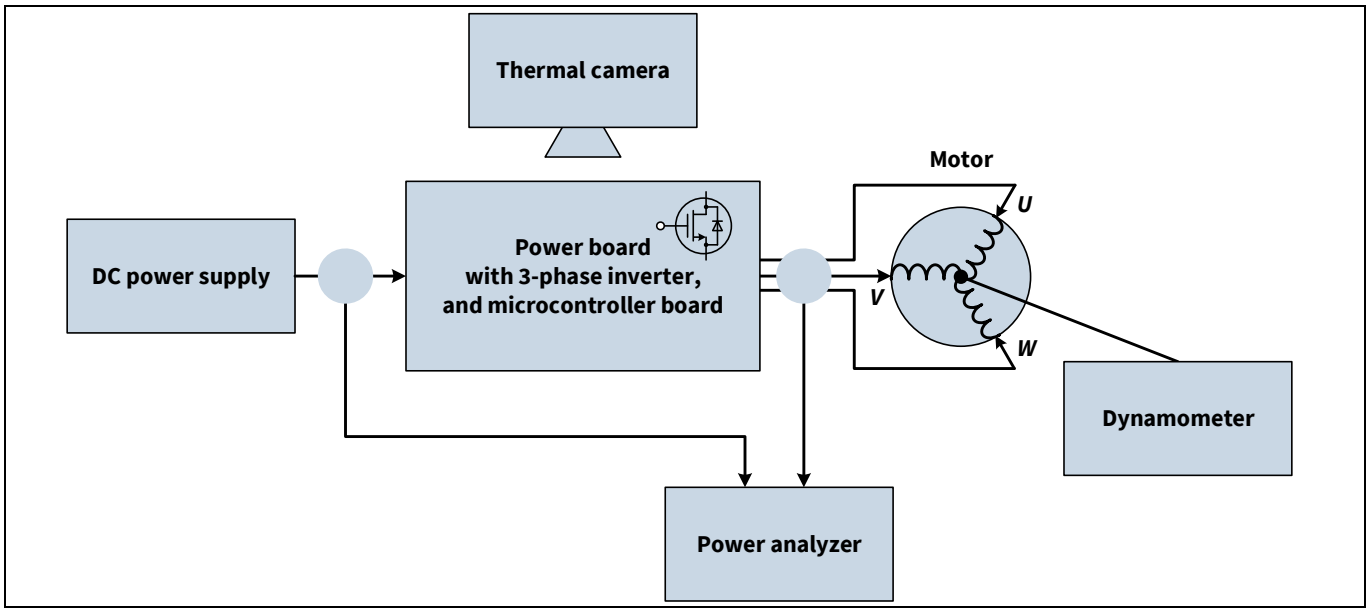

Figure 5 Test set-up

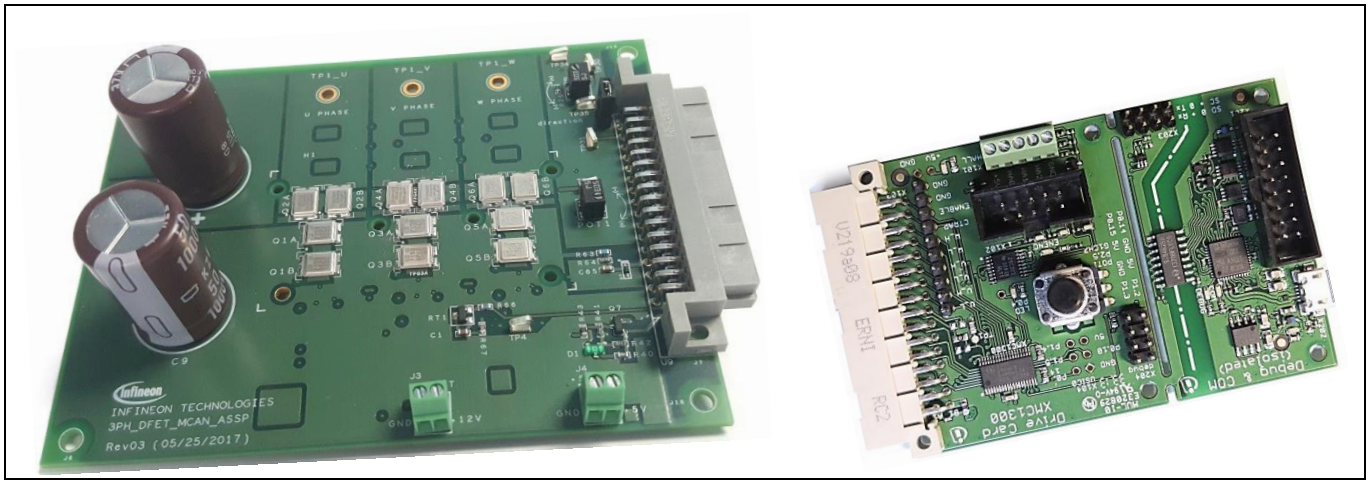

Figure 6 Power board with three-phase inverter (on the left) and microcontroller board (on the right)

Table 3 Parameters of three-phase BLDC motor in power tool

Nominal voltage [V]	Maximum motor speed [rpm]	Phase inductance [µH]	Phase resistance [mΩ]	Motor pole pair number	Gearbox ratio
18	26,000	16	1	2	1:48

4.2 Motor phase current comparison

An example waveform of the motor phase current for block commutation with Hall sensors is shown in Figure 7 (a), and for sensorless FOC in Figure 7 (b). The phase current observed in the block commutation case shows a typical trapezoidal shape, while for sensorless FOC a close to sinusoidal waveform can be seen. As mentioned before, the motor used has a trapezoidal distribution of windings, leading to not perfectly sinusoidal current waveform in the case of sensorless FOC.

For this example, high-side modulation with synchronous rectification is selected for block commutation. This means that the high-side MOSFET of each inverter phase switches with a complementary PWM on the low-side MOSFET for 120 degrees in each electrical revolution (i.e. 360 degrees). Synchronous rectification helps reduce the MOSFET body-diode losses, considerably reducing the power loss.

For this example, a five-segment SVM scheme is selected for sensorless FOC and the low-side MOSFET of each inverter phase remains on while the corresponding high-side MOSFET stays off for 120 degrees in each electrical revolution. Compared with the seven-segment SVM scheme, five-segment SVM reduces the MOSFETs' switching by one-third and helps reduce the MOSFET switching losses in sensorless FOC. More details of five- and seven-segment SVM schemes can be found in [5], and the seven-segment SVM scheme is not used for the test.

Due to the torque ripple at each commutation of the block commutation, the DC link bulk capacitor current shows higher ripple (3.95 A rms), while the bulk capacitor current for sensorless FOC is smoother and presents less ripple (3.18 A rms). This current ripple difference has an impact on the bulk capacitor power losses occurring due to the inherent capacitor Equivalent Series Resistor (ESR) that finally translates to a lower capacitor temperature.

Test results comparison

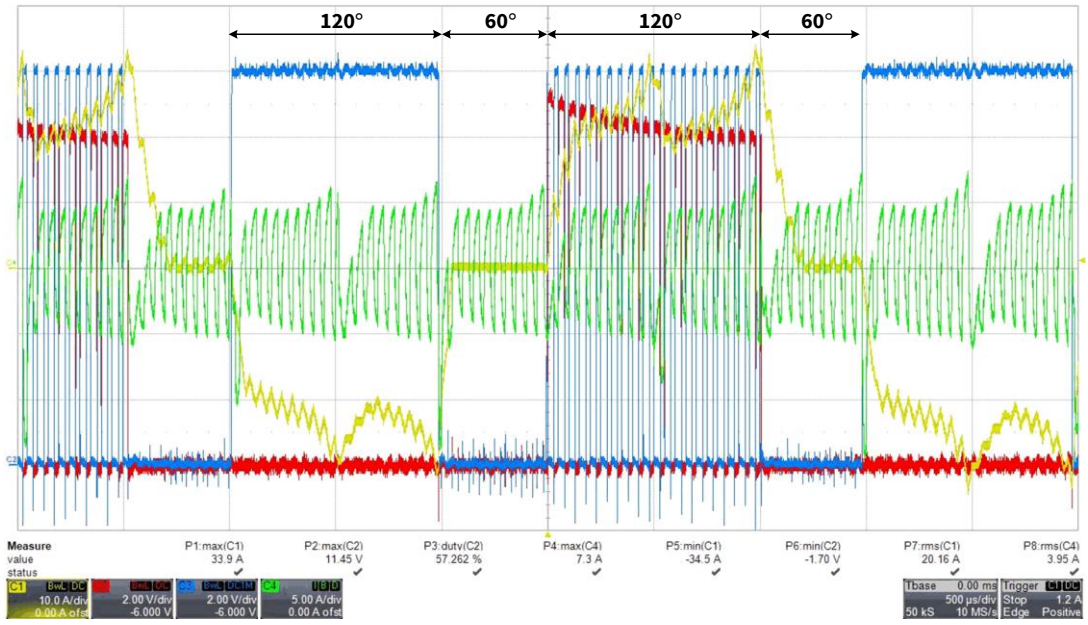

(a) Block commutation with Hall sensors

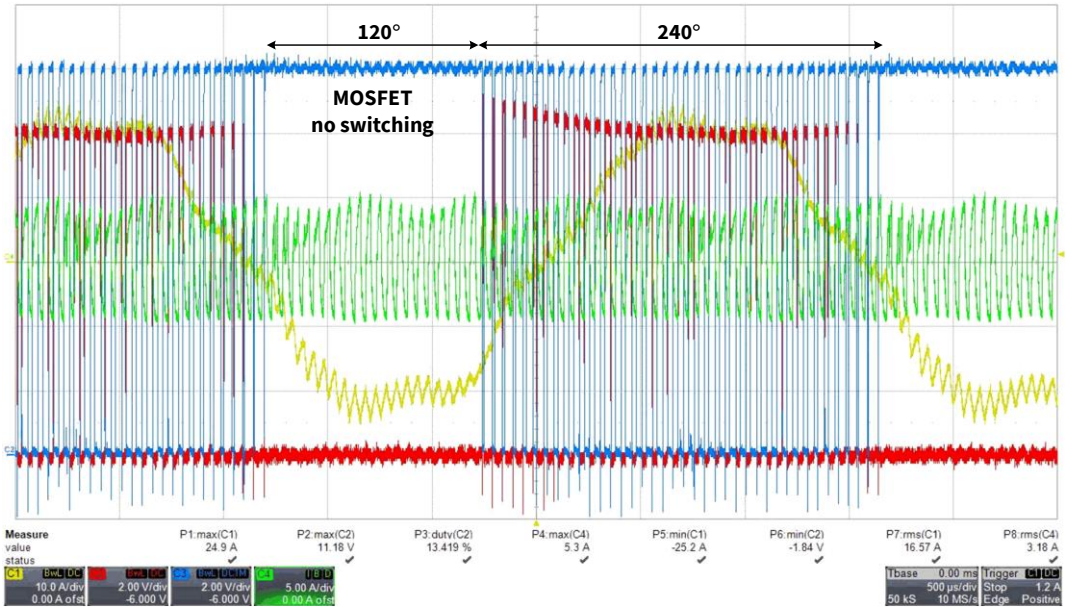

(b) Sensorless FOC

- CH1 (yellow) – I_u, motor phase U current from current probe (10 A/div)
- CH2 (red) – V_{GS_HS}, V_{GS} voltage of high-side MOSFET of inverter phase U (2 V/div)
- CH3 (blue) – V_{GS_LS}, V_{GS} voltage of low-side MOSFET of inverter phase U (2 V/div)
- CH4 (green) – I_{cap}, ripple current of one of the DC link bulk capacitors (5 A/div)

Figure 7 Waveforms of block commutation with Hall sensors and sensorless FOC

4.3 Power comparison

The test conditions for power comparison are listed in Table 4. The motor is run in both cases for the same duration, and measurements are done after thermal stabilization.

Test results comparison

Table 4 Test conditions for both block commutation and sensorless FOC

V DC [V]	Motor speed [rpm]	Shaft output torque [Nm]	Motor output power [W]	PWM frequency [kHz]	Dead-time [µs]
18	10,000	5.65	124	20	0.75

The results of the power analysis are presented in Table 5. For the same mechanical output power of the motor, the electrical output power of the board to the motor (i.e., the motor input electrical power) is lower for sensorless FOC, which means the motor is more efficient. The total power loss of sensorless FOC is also lower than in block commutation.

Table 5 Power comparison of block commutation and sensorless FOC

Item	Block commutation	Sensorless FOC	Comments
Motor shaft output power (W)	124	124	Mechanical output power
Power board output power (W)	208	196	Electrical power
Power board input power (W)	220	204	
Board power loss (W)	12	8	
Power board efficiency	94.5 percent	96.1 percent	

4.3.1 MOSFET power loss comparison

For the test conditions as listed in Table 4, the power loss breakdown [6] of high-side and low-side MOSFETs is shown in Figure 8.

The results are interpreted for the given conditions. Different conditions such as loading of the motor shaft, motor speed, MOSFET selection or switching frequency of PWM will impact for example the switching speed or the duty cycle of the MOSFETs, leading to a different ratio of losses. The selected conditions are relevant for the discussed application and should guide the reader in power loss comparison of both methods.

The main results are as follows:

- For both block commutation and sensorless FOC, the switching loss of the high-side MOSFETs is dominant. The high switching charge Q_{sw} ($Q_{sw} = Q_{gs2} + Q_{gd}$) of the power MOSFET IRF7480MTRPbF [7] is responsible for this high switching loss.
- Conduction loss has only limited relevance, especially in the high-side MOSFETs.
- Body-diode conduction losses are the key factor to improve in block commutation low-side MOSFETs, as they represent more than 60 percent of the losses.
- Body-diode losses are dramatically reduced in FOC as the low-side diode is not recirculating the current as in block commutation. This is more evident in the low-side MOSFET, where a reduction of 90 percent is seen.
- Switching losses in low-side MOSFETs are larger in FOC as the low-side MOSFETs switch more often.

Test results comparison

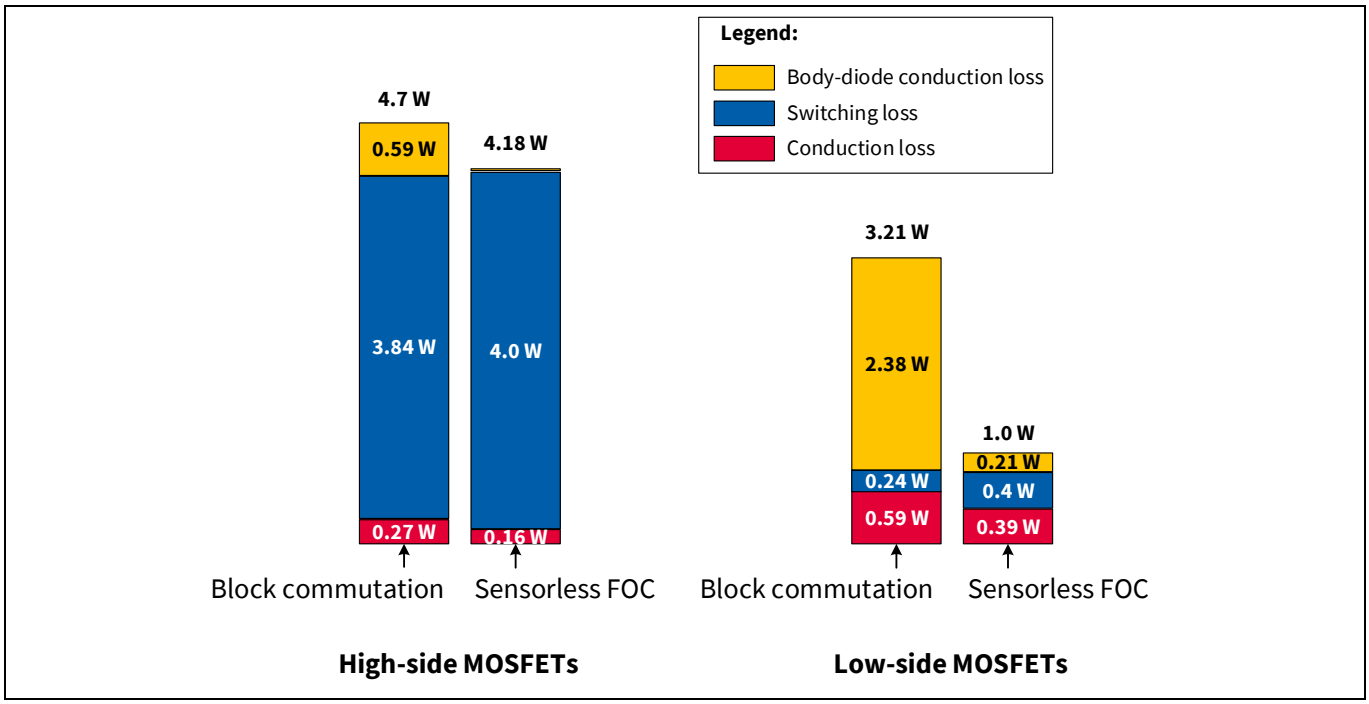

Figure 8 Power loss breakdown comparison for block commutation and sensorless FOC

In summary, high-side MOSFET power losses for sensorless FOC are about 10 percent lower than block commutation, but considerable lower – almost a 70 percent reduction – for low-side MOSFETs. Under the described conditions, total power losses on the power MOSFETs when utilizing sensorless FOC (about 5.2 W) are about 33 percent lower than block commutation losses (about 7.9 W), and the three-phase power inverter efficiency of sensorless FOC is therefore higher than BLDC block commutation.

4.4 Thermal comparison

For this example, the motor was run for the same test conditions and duration. After thermal stabilization is achieved, an image is captured with a thermal camera. The images are shown in Figure 9 with the same temperature scale. The maximum temperature of the board is 73.6°C for block commutation and 58.5°C for sensorless FOC. This is consistent with the measured lower power losses of the sensorless FOC. The FOC algorithm reduces the board temperature under the conditions described by 15.1°C.

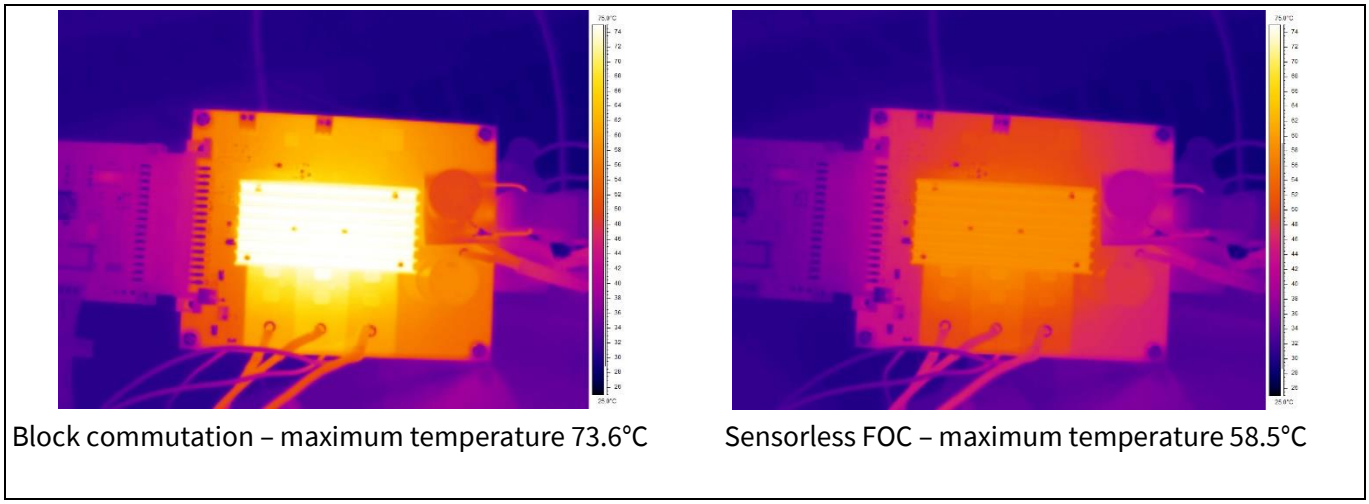

Figure 9 Thermal image comparison for block commutation and sensorless FOC

4.5 Motor start-up comparison

Improvements in algorithms and the support of higher processing power in new microcontrollers like XMC™ has simplified start-up of motors using sensorless FOC algorithms. A consistent and smooth closed-loop start-up of sensorless FOC can be achieved using the rotor position from the sensorless estimator mentioned in Section 3.2 and Section 3.3. Figure 10 compares the current waveforms of two examples of motor start-up: a) block commutation with Hall sensors and b) sensorless FOC.

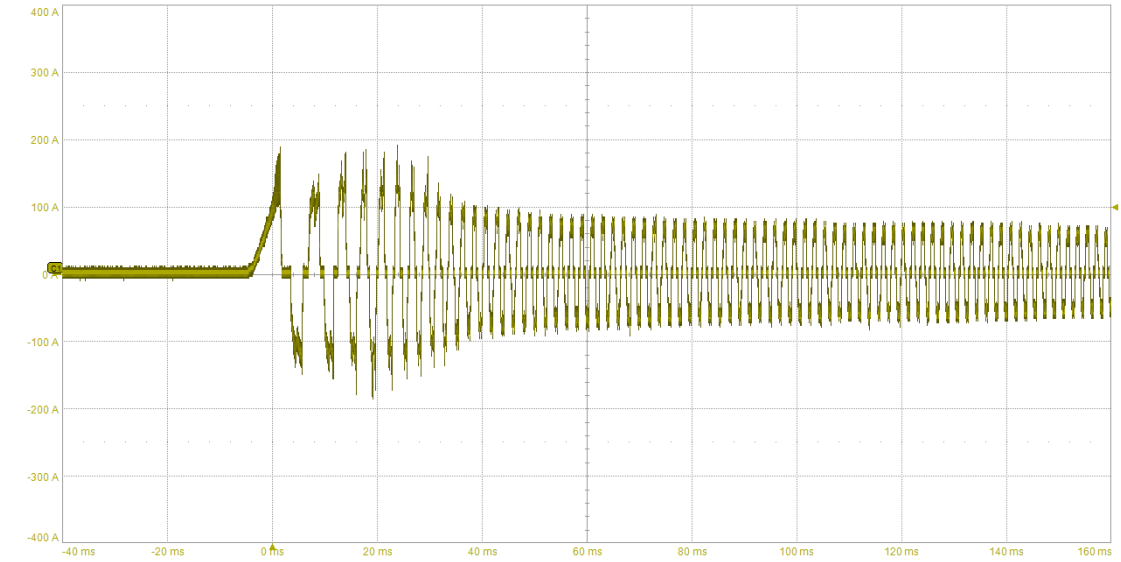

(a) Block commutation with Hall sensors

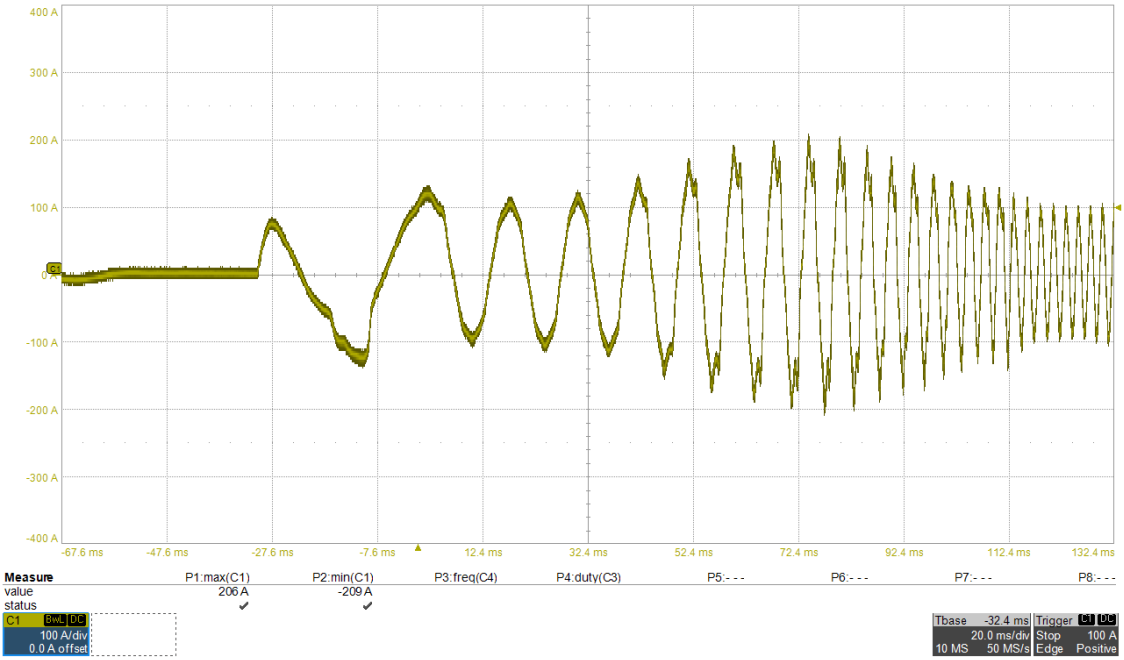

(b) Sensorless FOC

- CH1 (yellow) – motor phase current from current probe (100 A/div)

Figure 10 Start-up waveforms of block commutation with Hall sensors and sensorless FOC

5 Summary

Hardware, software and test results of BLDC block commutation with Hall sensors and sensorless FOC for three-phase BLDC motors in power tool applications have been compared.

Compared with BLDC block commutation with Hall sensors, sensorless FOC results in lower power losses and higher efficiency for the power board. To further reduce MOSFET power loss, for BLDC block commutation with Hall sensors it is desirable to choose MOSFETs with body-diode or low forward voltage (e.g. Infineon 40 V MOSFETs with integrated monolithic Schottky-like diode) as the body-diode conduction loss of MOSFETs is significant, while for sensorless FOC choosing faster switching silicon MOSFETs or gallium nitride (GaN) FETs will help to reduce the dominant switching loss.

The motor current of sensorless FOC is sinusoidal or close to sinusoidal depending on motor design. This will result in smoother motor output torque, which is beneficial to applications such as sanders and grinders for better polishing. It will also achiever quieter (acoustic) motor operation and fewer EMI problems than BLDC block commutation with Hall sensors.

The robust motor start-up of sensorless FOC is especially valuable, as load torque is often unknown or changing rapidly in power tool applications. By eliminating rotor sensors and their cables, connectors and PCBs, sensorless FOC is well-suited to power tool applications in harsh environments due to severe moisture, humidity, temperature or vibrations, or where conventional rotor sensors cannot be accommodated due to reliability concerns, cost or physical constraints.

6 References

[1] Infineon Technologies, Application Note AP32359, BLDC motor control software using XMC™, V1.0, January 2017.

[2] Infineon Technologies, Application Note AP32370, PMSM FOC motor control software using XMC™, V1.5, December 2018.

[3] Infineon Technologies, White Paper, Power loss and optimized MOSFET selection in BLDC motor inverter designs – understanding MOSFET power losses in block (trapezoidal) commutation, April 2016.

[4] Infineon Technologies and RWTH Aachen University, Motor Handbook, Version 2.1, March 2019.

[5] Wei-Feng Zhang and Yue-Hui Yu, Comparison of Three SVPWM Strategies, Journal of Electronic Science and Technology of China, Vol. 5, No. 3, September 2007.

[6] Hrach Amirkhanian and Steve Oknaian, Power Loss Breakdown in BLDC Drives Applications Using MATLAB, PCIM Europe 2018.

[7] Datasheet of IRF7480MTRPbF, Infineon, 2016-5-4.

Revision history

Document version	Date of release	Description of changes
V1.0	November 2019	Initial release

Trademarks
All referenced product or service names and trademarks are the property of their respective owners.

Edition 2019-11-06

Published by

Infineon Technologies AG

81726 Munich, Germany

© 2019 Infineon Technologies AG. All Rights Reserved.

Do you have a question about this document?

Email: erratum@infineon.com

Document reference
AN_1911_PL88_2001_203254

IMPORTANT NOTICE

The information contained in this application note is given as a hint for the implementation of the product only and shall in no event be regarded as a description or warranty of a certain functionality, condition or quality of the product. Before implementation of the product, the recipient of this application note must verify any function and other technical information given herein in the real application. Infineon Technologies hereby disclaims any and all warranties and liabilities of any kind (including without limitation warranties of non-infringement of intellectual property rights of any third party) with respect to any and all information given in this application note.

The data contained in this document is exclusively intended for technically trained staff. It is the responsibility of customer's technical departments to evaluate the suitability of the product for the intended application and the completeness of the product information given in this document with respect to such application.

For further information on the product, technology, delivery terms and conditions and prices please contact your nearest Infineon Technologies office (**www.infineon.com**).

WARNINGS

Due to technical requirements products may contain dangerous substances. For information on the types in question please contact your nearest Infineon Technologies office.

Except as otherwise explicitly approved by Infineon Technologies in a written document signed by authorized representatives of Infineon Technologies, Infineon Technologies' products may not be used in any applications where a failure of the product or any consequences of the use thereof can reasonably be expected to result in personal injury.